Effect of survey parameters on unmanned aerial vehicles-derived topography for coastal dune monitoring

Luísa Bon de Sousa,* **Susana Costas**, **and Óscar Ferreira**
University of Algarve, Centre for Marine and Environmental Research, Faro, Portugal

Abstract. Coastal dunes are fragile ecosystems emerging at the interface between marine and continental environments. They provide multiple services, among which are the protection against the impact of storms and the hosting of diverse and unique species of fauna and flora. However, changes in the topography or biological component of these systems may endanger the perpetuation of service provision. Topographic changes within dunes can significantly differ in magnitude depending on the type of process (i.e., marine or aeolian) and the temporal scale of analysis (event to annual scale), making their monitoring a challenging task. In recent years, unmanned aerial vehicles (UAVs) have been increasingly used to monitor coastal dunes, proving to be a cost-efficient methodology for the collection of topographic data. Yet, the application of UAVs in combination with the structure from motion approach to obtain digital surface models (DSMs) presents some limitations related to the level of accuracy provided for the evaluation of topographical changes in dunes with low sedimentation rates. This work explores different survey configurations using UAVs flying at low altitudes with the aim of obtaining high-quality DSMs with vertical accuracies preferably around or lower than 0.04 m. Several tests were performed to evaluate the influence of different parameters on the accuracy of the DSM, including flight altitude and orientation, density and spatial distribution of ground control points (GCPs), terrain slope, vegetation cover, and sun-related parameters. The results indicate that the intended accuracies can be obtained by combining overlapped perpendicular flights, GCPs distributed regularly following a diamond grid, with densities of at least 6 GCPs per hectare, sun altitudes between 30 and 40 deg, and a total solar radiation per hour between 1750 and 2250 KJ/m^2. In addition, better results were obtained across gentle slope areas, suggesting the eventual need to adapt to the particularities of each site to ensure the accuracy. [DOI: 10.1117/1.JRS.16.034513]

Keywords: vertical accuracy; ground control points; sun-related parameters.

Paper 220102G received Feb. 22, 2022; accepted for publication Jul. 13, 2022; published online Jul. 29, 2022.

1 Introduction

Coastal dunes provide a series of ecosystem services that include hosting endangered and highly specialized flora and fauna, protecting coastal infrastructure and properties from wave impact,[1,2] and offering significant recreational resources. Coastal dunes may undergo substantial topographical changes due to the impact of storm events, which may induce erosion by wave action, and the relevant accumulation of sediment by aeolian transport. Yet, dunes evolve at relatively large temporal scales (years to decades) due to the low sediment supply rates that characterize these environments.[3,4] The high relevance of these systems, from an ecological and defense point of view, explains the increasing number of monitoring programs focusing on coastal dunes and aiming to understand how these systems adapt and evolve over time.[5] In addition, their fragility and elevated morphological complexity explain the need for using remote sensing techniques that are non-intrusive and can provide high-resolution topographic maps.[6]

Some of the most commonly used methodologies to monitor coastal dunes include the airborne light detection and ranging (LiDAR) and the terrestrial laser scanner (TLS).[5] However, unmanned aerial vehicles (UAVs) have been increasingly used to monitor morphological

*Address all correspondence to Luísa Bon de Sousa, mlssousa@ualg.pt

changes in dynamic environments such as beaches and dunes.[7–9] UAVs combined with the structure from motion (SfM) approach allow for the elaboration of high-resolution topographic maps,[10,11] being a cost-effective survey tool that can provide high-quality data.[6–9,11–14] Several authors proved the suitability of UAVs for coastal dune monitoring by obtaining similar results and errors when comparing the topographic maps generated with this technique to alternative ones, such as TLS or airborne LiDAR.[11,15–18] These authors also highlighted the limitation of UAV products where vegetation is dense due to the inability of photogrammetric methods to map the ground surface below the vegetation, making it extremely difficult to obtain highly accurate digital terrain models (DTMs) in areas with dense vegetation.[19–22] Among the advantages of the use of UAVs, it has been found that the high degree of automatization associated with UAVs surveys allows for not only time-efficient data collection that is easily repeated over time but also the simultaneous collection of topographic and orthophoto map data, which allows for the coupled analysis of morphological and vegetation changes.[9,11,15,23,24]

The topographic products derived from UAV imagery may have a variable accuracy depending on survey configurations[19] and atmospheric conditions (e.g., sunlight and wind speed).[25] In this regard, atmospheric conditions need to be considered when planning the survey, with particular attention to wind speeds, solar radiation, and sun incidence. In addition, when planning a survey, it is highly relevant to evaluate the most appropriate flight altitude and orientation considering the survey area and the local legislation.[15,21] Another important aspect that can affect the accuracy of the results is the number and distribution of ground control points (GCPs). Different works aimed to define optimal GCP distribution for different study cases.[12,21,26] All of these studies highlight the importance of the GCPs number and distribution to maintain errors (vertical and horizontal) below 0.10 m, optimizing the total surveying time, which includes the time needed to deploy and collect the GCPs. For the particular case of dune systems, recent studies tried to find the best combination of flight altitude and GCPs density to optimize their results,[9,14,19,27] using flights from 30 to 80 m and GCPs spacing from a few tens of meters up to 250 m apart. The discrepancy in the suggested combinations of flight altitude and GCPs density is so high that it is difficult to identify and choose the best method to perform high accuracy surveys on dune.

The present work explores UAVs-SfM approaches to acquire high resolution and accurate topographic maps to monitor geomorphological features evolving at different temporal scales as is the case of coastal dunes. In this line, this work aims to identify the best combination of parameters relevant to the UAV-SfM survey to reduce vertical errors and improve the accuracy of UAVs-SfM products that can be easily replicated at any coastal dune area and other environments with similar characteristics and where high accuracy is desired. For that, a series of tests was performed to evaluate the effect of different survey configurations (e.g., UAVs flight altitude and orientation, and GCPs distribution and number), sun-related parameters (e.g., sun altitude and azimuth, and solar radiation), and dune slope and vegetation cover on the UAV-SfM product accuracy. The tests were performed at the coastal dune of Ancão Peninsula, located in South Portugal.

2 Materials and Methods

2.1 *Study Area*

The coastal dune selected to carry out the tests and explore the best UAVs-SfM approach in terms of products accuracy is located at the eastern part of the Ancão Peninsula (Fig. 1). Ancão Peninsula belongs to the multi-inlet barrier island system of Ria Formosa, South Portugal [Fig. 1(a)]. The area selected to carry out the tests has shown shoreline progradation in recent decades,[28,29] enhanced after inlet relocation in 1997, and subsequent accumulation of sand within the updrift area.[30] According to Costas et al.,[31] the rate of aeolian sediment transport and accumulation in the area is relatively low because of a combination of factors, among which are the coarse nature of the sand, the relatively low wind intensity, and the existence of erosive features associated with the impact of storms.

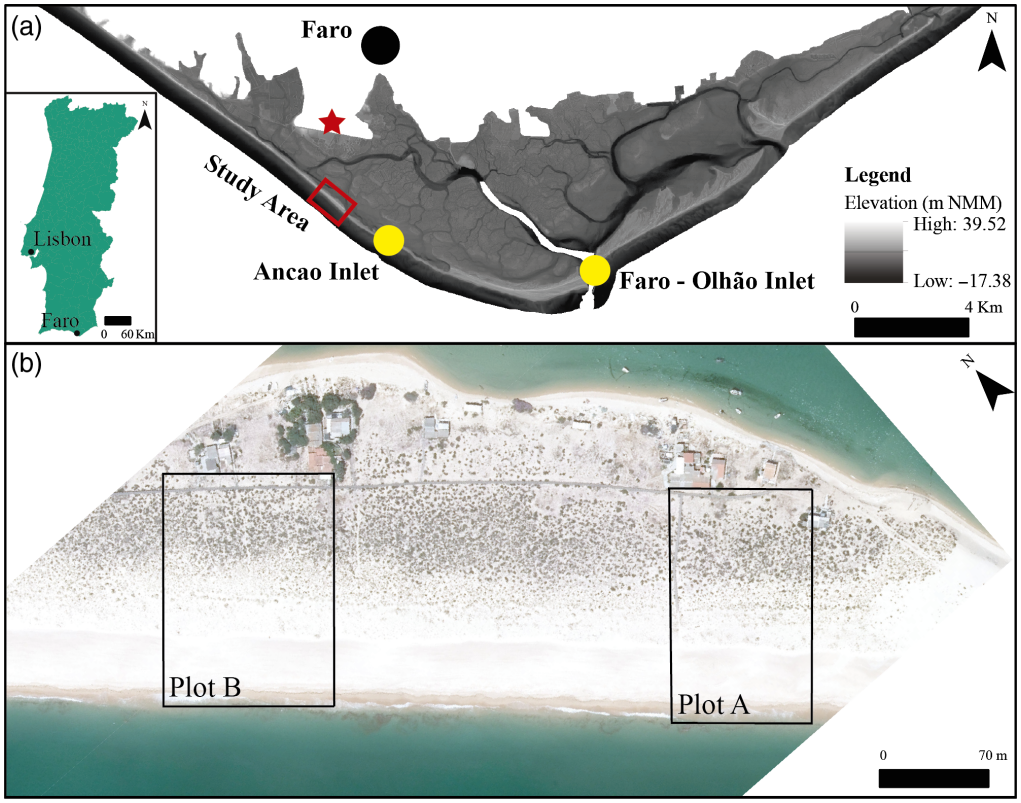

Fig. 1 (a) Ria Formosa Barrier Island System, South Portugal (source: LIDAR 2011, Direção Geral do Território). The red rectangle shows the location of the study area, at the eastern part of the Ancão Peninsula, the red star is the location of the airport, and the yellow circles are the locations of Ancão Inlet and Faro-Olhão Inlet. (b) Vertical image of the study area showing the plots where the tests were performed.

This area is within a flight restriction zone to UAV flight altitude due to the proximity to the Faro Airport, which restricts flights to low altitudes. The experiments carried out consisted of the survey of two plots of around 120 × 100 m [Fig. 1(b)], covering the total width of the dune ridge and separated 200 m apart alongshore. Plot A has a total area of 1.62 ha, and plot B has a total area of 2.04 ha. The surveyed plots differ morphologically and topographically across-shore and include an incipient dune and a fixed dune ridge. The incipient dune is located at the seaward part with an average elevation of around 5.2 m above mean sea level (MSL) and is characterized by low vegetation densities (below 20%). The plant community is dominated by *Eryngium maritimum*, *Elymus farctus*, *Medicago marina*, and very small patches of *Ammophila arenaria*.[32] The fixed dune ridge has a maximum elevation of around 7 m above MSL and is characterized by higher vegetation densities (above 60%), dominated by *Artemisia crithmifolia* and *Medicago marina*.[32] The lee side of the dune ridge represents the transition to the back-barrier area and is characterized by vegetation densities of about 50%, dominated by *Artemisia crithmifolia*.[32] These morphological regions allow for dividing the plots across-shore into four sections according to their topography (Fig. 2). Sec. 1 represents the lee side of the dune ridge, dipping gently inland; Sec. 2 represents the crest of the dune ridge (elevations >6 m); Sec. 3 represents the stoss slope of the dune ridge, gently dipping seaward; and Sec. 4 covers the incipient dune and the beach backshore.

2.2 *General UAV-SfM Characteristics*

A Mavic 2 Pro UAV from DJI equipped with a Hasselblade L1D-20c Camera (Table 1), was used to obtain the images of the plots. The UAV was flown in an autonomous mode using DroneDeploy or DJI GSP mission planner, with frontal and side overlaps of 80% and 75%,

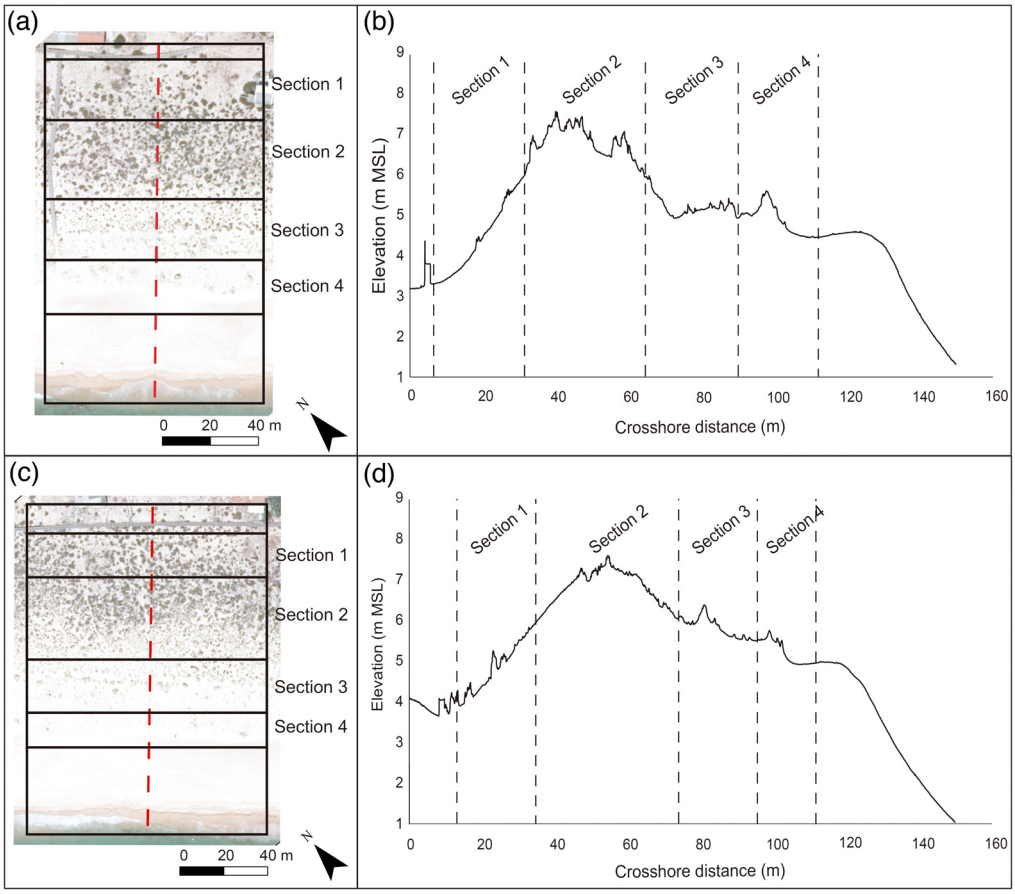

Fig. 2 (a) Vertical image of plot A showing Secs. 1–4. (b) Topographic profile corresponding to the location of the red dashed line in A. Vertical dashed lines represent the limits of the cross-shore sections. (c) Vertical images of plot B showing Secs. 1–4. (d) Topographic profile corresponding to the location of the red dashed line in C. The dashed lines represent the limits of the sections.

Table 1 Specifications of the UAV used.

UAV model	Mavic 2 pro
Sensor	1" CMOS
No of pixels	20 MP
Lens	FOV: about 77 deg
	35-mm format equivalent: 28 mm
	Aperture: $f/2.8 - f/11$
	Shooting range: 1 m to ∞
Flight planning and control software	Drone deploy and DJI GSP

respectively. The ground sampling distance (GSD) defines the spatial resolution or pixel size of the UAV-SfM products, which depends on the UAV camera, flight altitude, and image overlap. The GSD values of each flight are automatically calculated by the mission planner (Table 2). The flights were performed between 10 am and 4 pm to minimize the shadow effect. The take-off for all tests was at the beach backshore, with a take-off altitude around 4 m above MSL. In terms of weather conditions, all flights were performed on a sunny day with calm winds up to light breeze (Beaufort Scale).

Table 2 Settings of each survey, flight, and associated tests.

Survey	Flight	Test	Plot	Flight orientation[a]	Flight altitude AGL[b] (m)	Average GSD[c] (cm)	Number of images	GCPs	GCPs density per ha	vRMSE (m)	Z error (m)
Sep 2019	S1	S1	A	Cross-shore	25	0.53	319	11	7	0.08	0.02
	S2	S2	B	Cross-shore	25	0.57	373	16	8	0.04	0.02
Jan 2020	J1	J1a	B	Cross-shore	40	0.86	159	17	8	0.03	0.02
	J2	J2	B		25	0.52	342	16	8	0.05	0.04
	J3	J3	B		30	0.69	273	17	8	0.03	0.03
	J1+J2	J4	B		25 + 40	0.63	501	16	8	0.03	0.03
May 2020	M1	M1	A	Cross-shore	30	0.68	280	7	4	0.09	0.02
	M2	M2	B		30	0.66	267	13	6	0.06	0.02
June 2020	JN1	JN1	A	Cross-shore	30	0.67	303	10	6	0.10	0.04
	JN2	JN2	A	Longshore	30	0.68	316	10	6	0.06	0.006
	JN1+JN2	JN3	A	Cross and longshore	30	0.67	619	10	6	0.04	0.002
Oct 2020	O1	O1	A	Cross and longshore	30	0.69	603	10	6	0.04	0.005
	O2	O2	B	Cross and longshore	30	0.69	552	9	4	0.07	0.004

[a]orientation relative to the coastline
[b]above ground level
[c]ground sample distance

Fig. 3 Example of a GCP target fixed on sand.

Before each flight, a set of GCPs was distributed within each plot. Each GCP consisted of a 30×30 cm black/brown standard target, with a central hole for insertion of a stack that secures the GCP to the ground (Fig. 3). The position and elevation of the central point of each target were measured using a DGPS-RTK with a horizontal and vertical accuracy of 0.011 and 0.017 m, respectively. In terms of time consumption, each flight took around 20 min, and the time needed to distribute, measure, and collect the GCP targets was around 2 h for each plot site.

An SfM approach was used to create digital surface models (DSMs) and orthophoto mosaics for all UAV tests performed. The images collected during the surveys were imported into the software Agisoft Metashape[33] and aligned using the metadata of each photo recorded during the survey (Fig. 4). Once the images were aligned, the GCP positions were imported into the software and manually verified in at least three different images to rectify the georeferentiation. After the images were georeferenced, a point cloud with ca. 6000 points/m^2, a DSM, and an Orthophoto mosaic were generated for each test, and the accuracy of these results was assessed by computing associated vertical root mean square errors (vRMSE) (Fig. 4).

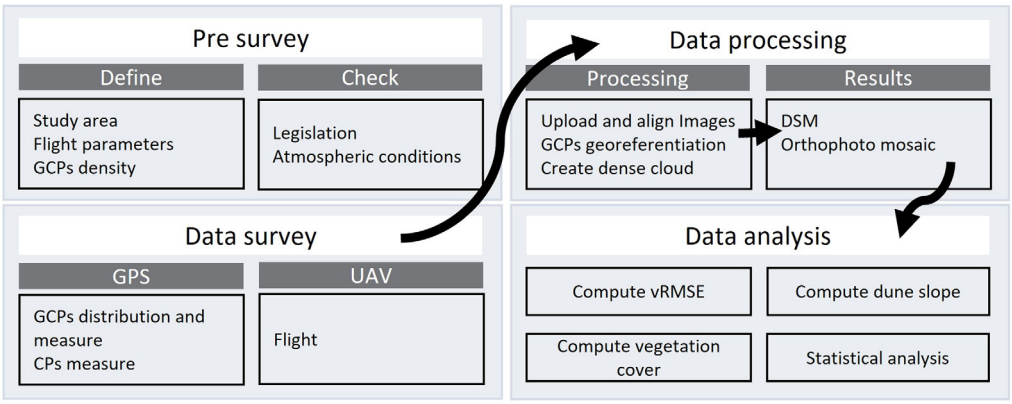

Fig. 4 Workflow of data surveying, processing, and analysis.

2.3 *Survey Design*

Five surveys were carried out on different days in September 2019, January 2020, May 2020, June 2020, and October 2020. During these surveys, five flights were performed at plot A and six at plot B. Each individual flight corresponded to a test, and some flights were combined into a new compound test (see Table 2). Tests differ one from the other by having different flight altitudes, flight orientations, GCPs (number and distribution), or sun-related parameters (see Tables 2–4). A total of 20 tests (Tables 2 and 3) was carried out and analyzed to evaluate (i) the influence of flying at different altitudes (test J1a, J2, J3, and J4) and orientations (test JN1, JN2, and JN3), (ii) the effect of changing the GCPs density and distribution (test J1a to J1h), and (iii) the effect of sun-related parameters, vegetation cover, and dune slope. The latter was done considering the tests with the best results from each of the 11 flights (Table 4).

The software used to obtain the DSMs allows for obtaining the vertical error (z error) for each test performed (Table 2). However, because of the lack of clear information about how this error is computed, these errors were not used as indicators of the vertical accuracy of each obtained DSM. Alternatively, an additional set of points (i.e., 50 points) across each plot was measured during each survey to be used as control points (CPs) supporting the calculation of the vertical accuracy. The CPs were measured with the DGPS-RTK over the dune surface following a regular grid and having the same accuracy as the GCPs.

2.3.1 *Flight settings and GCP distribution*

To understand the influence of flying at different altitudes, three flights were performed at altitudes between 25 and 40 m in January 2020 at plot B (J1 to J3, Table 2). Additionally, the effect of combining two flight altitudes was assessed by overlapping the images collected at 25 and 40 m (test J4, Table 2).

Two flights were performed at an altitude of 30 m during the survey performed in June at plot A to evaluate the influence of flight orientation on the accuracy of the products (test JN1 and JN2, Table 2). The flights were oriented relative to the coastline, alongshore and across-shore. Additionally, the effect of combining two flight orientations (i.e., longshore and cross-shore) was assessed (test JN3, Table 2).

The influence of the GCPs density and distribution was evaluated using the images acquired during flight J1 (Table 3). For that, new projects were created in AGISOFT using alternative combinations (density and distribution) of GCPs (Table 3 and Fig. 5).

Table 3 Settings of the tests performed to evaluate the influence of the GCPs number and distribution.

Survey	Flight	Test	Plot	Flight orientation[a]	Take-off AGL[b] (m)	Average GSD[c] (cm)	Number of images	GCPs	GCPs density per ha	vRMSE (m)
January 2020	J1	J1a	B	Cross-shore	40	0.86	159	17	8	0.03
		J1b						13	6	0.04
		J1c						12	6	0.04
		J1d						11	5	0.03
		J1e						9	4	0.04
		J1f						7	3	0.04
		J1g						5	2	0.09
		J1h						4	2	0.20

[a]orientation relative to the coastline
[b]above ground level
[c]ground sample distance

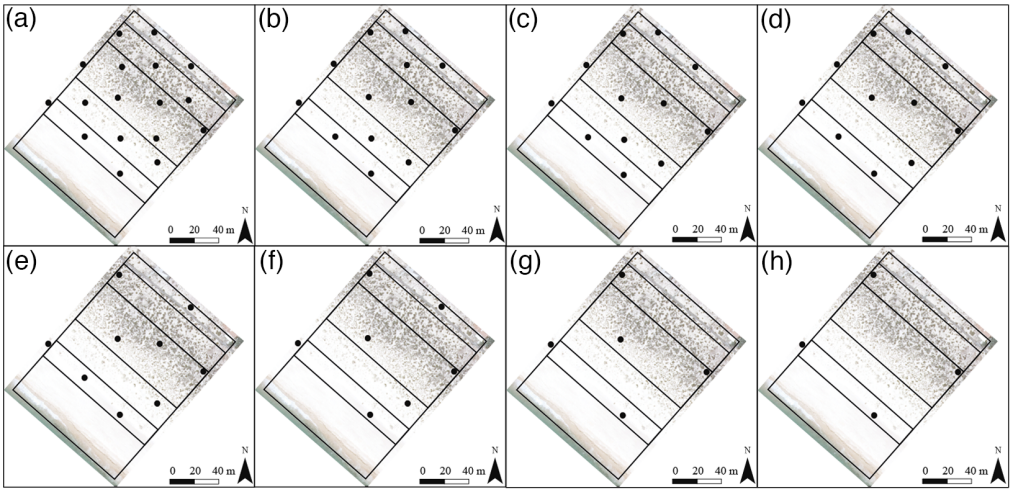

Fig. 5 Distribution of the GCPs within plot B in January 2020. (a) Test J1a; (b) Test J1b; (c) Test J1c; (d) Test J1d; (e) Test J1e; (f) Test J1f; (g) Test J1g; and (h) Test J1h. See Table 3 for characteristics of each test.

The influence of changing the flight settings or GCPs was assessed by comparing the vRMSEs from all tests.

2.3.2 *Sun-related parameters*

The sun position (altitude and azimuth) and the solar radiation are external parameters that may influence the vertical accuracy of the products from the UAV-SfM approach. The information regarding sun position was consulted and retrieved from the website[34] for the start time of each flight (Table 4). Regarding solar radiation, the value of the total solar radiation per hour was used to characterize this parameter during the time of each flight (Table 4). For that, the data recorded at the Faro Airport meteorological station and provided by Instituto Português do Mar e da Atmosfera (IPMA) were used (Fig. 1). The influence of these parameters on the vertical accuracy was evaluated by assessing the statistical significance of the relationships between each parameter and the vRMSE for all performed tests. For that, the Spearman correlation coefficient (rho (r)), which is a nonparametric statistical measure of the strength of a monotonic relationship

Table 4 Sun-related parameters for each flight.

Survey	Flight	Plot	Flight time	Sun altitude (deg)	Sun azimuth (deg)	Total solar radiation (KJ/m^2 per hour)
September 2019	S1	A	14h20	53.23	202.73	2956
	S2	B	16h12	38.82	237.79	2102
January 2020	J1	B	11h30	29.21	161.21	1462
	J2	B	11h40	29.81	163.79	1462
	J3	B	11h59	30.71	168.80	1462
May 2020	M1	A	13h17	73.16	170.63	3413
	M2	B	15h39	57.15	248.67	2974
June 2020	JN1	A	10h00	42.44	90.82	2653
	JN2	A	10h14	45.23	93.02	2653
October 2020	O1	A	15h55	28.69	225.48	1476
	O2	B	10h41	29.27	135.31	2080

between paired data, was estimated for each correlation. The correlations were considered significant for a 95% or higher confidence level.

2.3.3 *Vegetation cover and dune slope*

The influence of the vegetation cover on the quality of the DSM was analyzed based on the results from 9 tests (S1, S2, J1a, J2, M1, M2, JN3, O1, and O2; see Table 2 for dates and characteristics of each test). The vegetation cover was estimated and quantified using orthophoto mosaics. The latter was classified into two classes to separate the vegetation (darker colors) and sand (lighter colors) using the unsupervised classification method in ArcGIS 10.8. Once the maps were classified, the vegetation cover, in percentage, was calculated for each section and test.

The slope of the dune was also considered to be a possible factor influencing the quality of the DSM. To evaluate the effect of the dune slope, cross-shore profiles were extracted every 10 m from each obtained DSM. The profiles were divided by the sections (see Fig. 2), and the average slope within each section was estimated.

The influence of these two parameters (vegetation cover and dune slope) on the vertical accuracy of the obtained DSMs was evaluated by analyzing the relationships between the values for these parameters and the corresponding vRMSEs calculated for each section. Simple linear regression analyses were performed, and the Pearson correlation coefficient (r) was estimated for each regression. The relationship between the variables and the vRMSE was considered significant for a 95% or higher confidence level.

3 Results

The total number of tests and, thus, of DSMs and orthophoto mosaics was 20. The number of images used for each test ranged between 159 and 619, which depended on the flight altitude and the overlap of flights (Table 2). The GSD varied between 0.52 and 0.86 cm, depending also on the flight altitude, with the lower value associated with a lower flight altitude (Table 2). The vRMSEs of the evaluated tests ranged between 0.03 and 0.20 m, with 60% of the values between 0.03 and 0.05 m (Tables 2 and 3), and significant spatial variation. The estimated vRMSE was about one order of magnitude greater than the one computed by the software, which ranged between 0.002 and 0.04 m (Table 2). According to the obtained values and their variability range, vRMSE was considered to be high accuracy for values smaller than 0.04 m, good accuracy for values between 0.04 and 0.07 m, reasonable accuracy for values between 0.07 and 0.10 m, and poor accuracy for values >0.10 m.

3.1 *Flight Parameters and GCP Distribution*

The tests performed to evaluate the effect of flying at different altitudes indicate that the vRMSE increases from 0.03 to 0.05 m as the altitude decreases from 40 to 25 m (Table 2, tests J1a and J2, respectively). If the images from both flights are combined, the vRMSE is the same as flying at 40 m (Table 2, test J4). Flying at an intermediate altitude (30 m) gave the same result as flying at 40 m (Table 2, test J3).

Regarding flight orientation, flying across-shore (vRMSE 0.10 m, test JN1, Table 2) generates greater vRMSE than flying alongshore (vRMSE 0.06 m, test JN2, Table 2). Yet, the vertical error was reduced (vRMSE equal to 0.04) when both flights were combined and overlapped (test JN3, Table 2).

In terms of GCPs density and distribution, the vRMSE did not show relevant changes when the number of GCPs was reduced from 17 to 7, showing an increase of only 0.01 m (test J1a to J1f, Table 3). However, the tests with <5 GCPs (test J1g and J1h, Table 3) were associated with vRMSE above 0.09 (Table 3). Reducing the number of GCPs changed not only their density but also their distribution (Fig. 5 and Table 3). Initially (test J1a), the distribution followed a diamond grid with a density of 8 GCPs per ha. However, this distribution could not be maintained when the density was reduced to 2 GCPs per ha (test J1g and 1h, Table 3), with only GCPs at the edges and one in the center of the flight area, which caused the increase of the vRMSE (Table 3).

3.2 *Sun-Related Parameters*

The solar radiation and the sun altitude and azimuth depend on the hour and day of the flight. In the region where the tests were performed, the maximum solar radiation normally occurs between 11 am and 1 pm, changing according to the time of the year. During winter, the maximum solar radiation can be similar to the solar radiation that characterizes the early morning or late afternoon during summer. For the performed flights, the solar radiation per hour varied between 1462 and 3413 KJ/m^2, respectively, for January 2020 at 11 am and May 2020 at 1 pm (Table 4).

The sun altitude and azimuth showed greater daily variations during the summer months than during the winter months. For the flights performed, the maximum sun altitude was 73 deg and the minimum 28 deg, corresponding to the flights carried out in May 2020 at 1 pm and in October 2020 around 4 pm, respectively (Table 4). The sun azimuth varied between 90 and 248 deg for the flights carried out in June 2020 at 10 am and May 2020 around 1 pm (Table 4).

The correlation between these parameters and the vRMSEs suggests that the variables were dependent except for the sun azimuth (Fig. 6). In general, when the total solar radiation per hour was higher than 2250 KJ/m^2, the vRMSE was higher than 0.06 m. For sun altitudes above 45 deg, the vRMSE was higher than 0.06 m, with better accuracies being obtained for sun altitudes between 30 and 40 deg. The tests performed with total solar radiation per hour below 1500 KJ/m^2 and sun altitudes below 30 deg show high variability in the values of vRMSE,

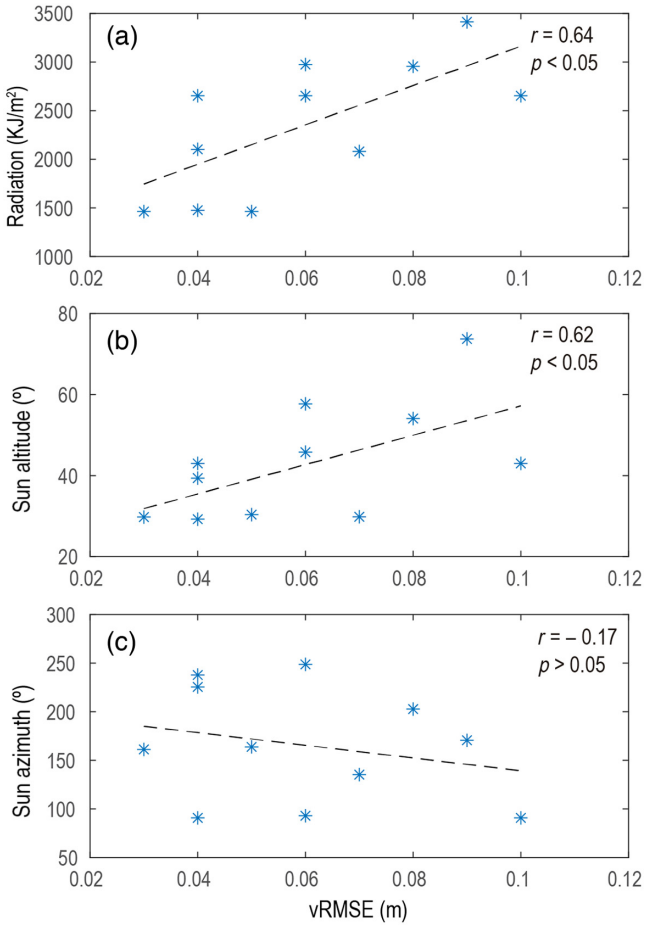

Fig. 6 Authors: the legend could be changed to: Relations between the vRMSE and different sun parameters, including total solar radiation (a), sun altitude (b) and sun azimuth (c). The results from the fitting between the different parameters and the vRMSE applying a non-parametric Spearmen correlation are given within each graph.

yet surveys were rarely performed under such conditions because of the associated very low light conditions.

3.3 *Vegetation Cover and Dune Slope*

The vRMSEs computed per dune section ranged between 0.02 and 0.16 m in plot A (Fig. 7) and between 0.02 and 0.09 m in plot B (Fig. 8). The vRMSEs in Sec. 3 were less variable for both plots, ranging between 0.05 and 0.09 m in plot A and between 0.03 and 0.09 m in plot B (Figs. 7 and 8).

For the case of plot A, maximum values of vegetation cover were recorded in October 2020, and minimum values were observed in September 2019 (Fig. 7). In plot B, maximum values were observed in May 2020, and minimum values depended on the evaluated section rather than on the survey day, e.g., Sec. 1 showed a minimum value in September 2019, and in Sec. 2 the minimum values were recorded in January and October 2020 (Fig. 8). The lower values of vegetation cover were found in Sec. 4, for both plots, representing the transition between the foredune and the backshore (Figs. 7 and 8). The relationship between vegetation cover and average vRMSE, per section, indicates that neither variable was related [Fig. 9(a)].

The mean dune slope per section was greater in Sec. 1, decreasing toward the sea in both plots. In plot A, the dune slope ranged from 0.02 to almost 0.15, whereas in plot B, it ranged from 0.02 to circa 0.11. The dune slope and the vRMSE, per section, were significantly related ($p < 0.01$), even though the correlation between both explained only 22% of the total variance [Fig. 9(b)].

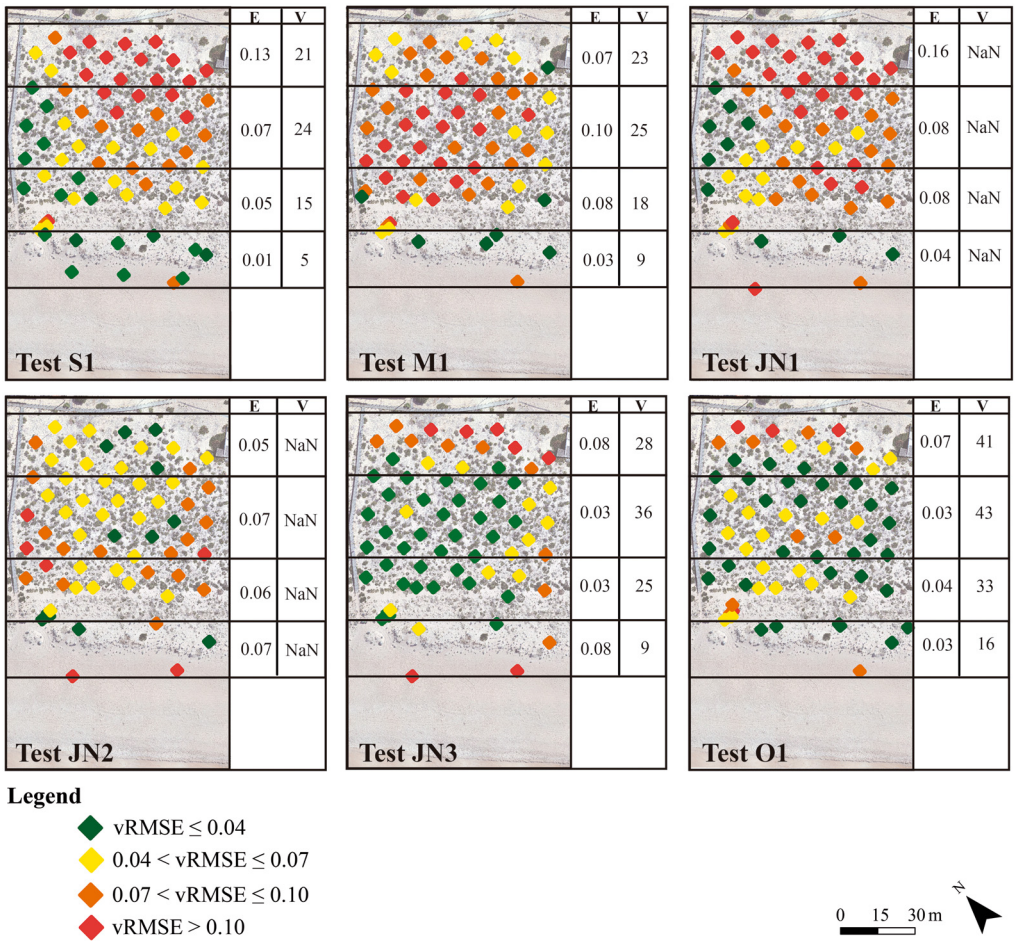

Fig. 7 Spatial distribution of vRMSE (m) in plot A. Values in column E represent the mean vRMSE per section, and values in column V represents the percentage of vegetation cover per section. See Table 2 for the dates and characteristics of each test.

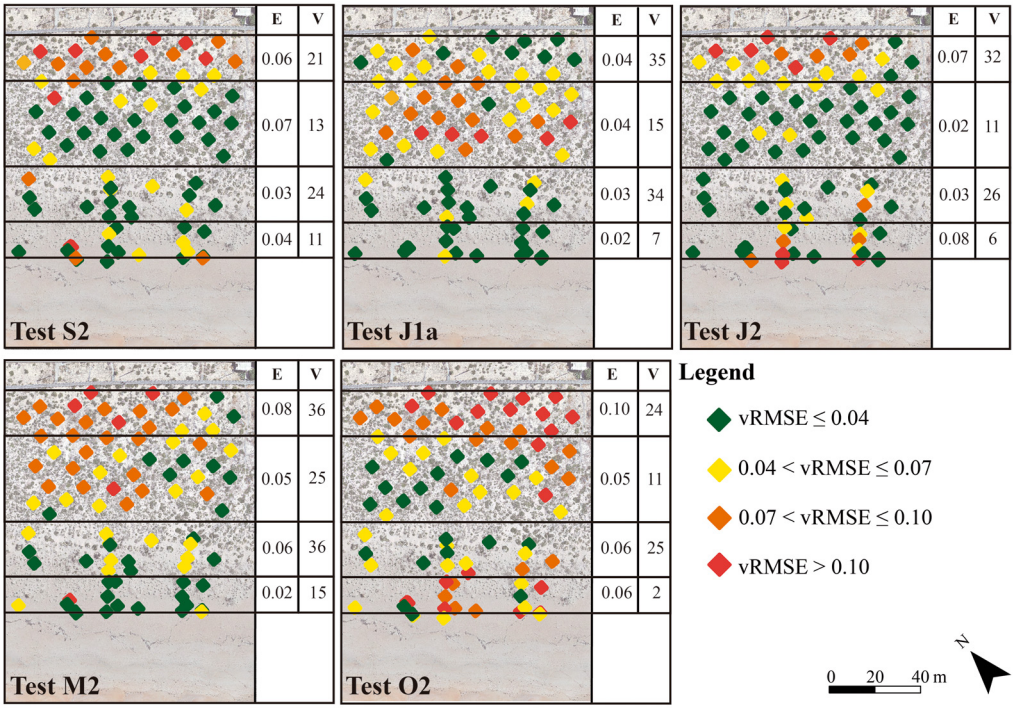

Fig. 8 Spatial distribution of vRMSE (m) in plot B. Values in column E represents the mean vRMSE per section, and values in column V represents the percentage of vegetation cover per section. See Table 2 for the dates and characteristics of each test.

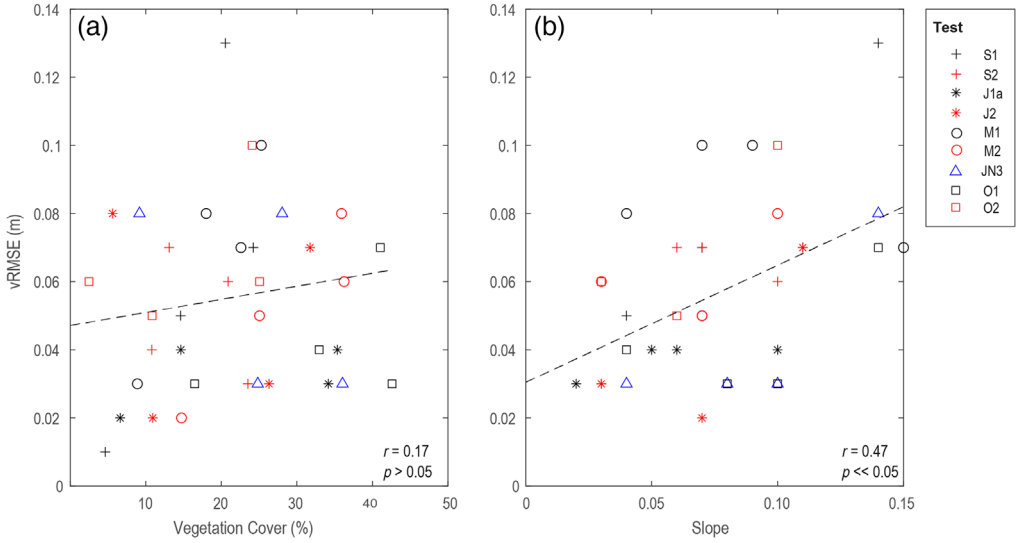

Fig. 9 (a) Relationship between vegetation cover and (b) dune slopes with the average vRMSE using data from all sections and tests. See Table 2 for the dates and characteristics of each test.

4 Discussion

The accuracy of the products obtained using UAVs depends on a series of factors involved in the whole process of data collection and processing, including flight altitude and orientation, density and distribution of GCPs, sun-related parameters, and dune slope. The present work investigated the effect of these factors on the vRMSE of the topographic maps obtained to maximize the

quality of the results for low-altitude flights. For that, this work explored the impact of the use of different flight configurations on the accuracy of the results to define an UAV-SfM approach that ensures the acquisition of topographic maps with high quality to monitor coastal dunes over time. The accuracy of the maps was assessed through the values of the obtained vRMSE, which should be kept low, preferably around or lower than 0.04 m, to capture small-scale morphological changes that often characterize coastal dunes; however, values up to 0.10 m were considered acceptable. This approach can also be applied to other environments where small morphological variations occur and need to be analyzed as, e.g., gully and soil erosion and small mass movements.

The use of UAVs to obtain topographic maps, orthophoto mosaics, or vegetation index maps has increased in recent years.[8] One of the main advantages of the use of UAVs is the low cost and rapid survey and processing times compared with other methodologies (e.g., airborne LiDAR or TLS). These advantages also permit the collection of data or monitoring with high frequency (i.e., monthly and seasonally) and high resolution (on the order of centimeters). The increase of the use of UAVs in the monitoring of coastal areas has promoted the discussion of the overall data collection design to ensure high accuracy results that meet the needs of the monitoring taking into account the particularities of the environments (e.g., different rates of change and complex morphologies). Yet, most works do not clearly explain how the quality of the obtained data is assessed, omitting details regarding the process of computing errors. Some works appear to adopt the error from the processing software, which tends to underestimate the actual error, whereas other works use CPs to compute errors but do not explicitly indicate how many CPs they used or their distribution. In the present work, the assessed error was obtained using CPs; the latter was very different from the software estimated errors, with differences up to one order of magnitude. One example of this is test JN3; its software-derived vertical error was 0.002 m, whereas the vRMSE estimated using CPs was 0.04 m. This suggests that the use of CPs is preferable for defining the quality of the results as it appears to give a more realistic result. The underestimation of the error by the software appears to be related to the use of the same points for error estimation and georeferencing of the images. Assuming that the vRMSE given by the software is correct would have very important consequences on the interpretation of the collected data, deriving unrealistic conclusions that are not representative of actual morphological changes. Moreover, to help understand the error distribution among the surveyed area, the CPs should cover the whole area. The ambiguity around this information in most published works makes it very difficult to compare the quality of the results among different works and even to understand if the obtained results do represent actual morphologic changes.

Most of the studies on monitoring coastal dunes using UAVs were performed flying between 60 and 100 m[8,9,35] and obtained variable mean accuracies ranging between 0.03 and 0.05 m, demonstrating that there is not a simple relation between accuracy and flight altitude. The present work supports the results from Taddia et al.[7] who found that high accuracies can be also obtained flying at low altitudes (around 30 m), depending on the flight settings. In this regard, the results suggest that a strategy to ensure data quality includes the overlap of two flight surveys using perpendicular flight orientations, which appear to improve significantly the accuracy of the topographic map.[36] Taddia et al.[36] observed that, with the use of perpendicular flight orientations and a tilt of the camera, the topographic maps have better accuracy when compared with a single flight using a camera in the nadir position. In this study, it was observed that the vRMSE can be reduced from 0.10 to 0.04 m when two flights at low altitudes with perpendicular orientations were overlapped (Table 2). The overlap of both flights allows for decreasing the influence of the shadows and seeing the same object in each image with different perspectives, permitting a better final accuracy.

Good accuracies result not only from the selected flight altitude (and orientations) but from a combination of additional factors, among which the density and distribution of GCPs appear to have a great impact. This study shows that better results can be obtained with GCPs distributed regularly following a diamond grid and covering the whole area (Table 3 and Fig. 5). Previous works found that stratified[35] and parallel[37] distributions helped to obtain good accuracies (0.04 to 0.07 m) flying at a range of altitudes (30 to 120 m). In terms of density, this study shows that better accuracy was found for densities ranging between 3 and 8 GCPs per ha (Table 3); however, densities below 6 GCPs per ha did not maintain a regular distribution of GCPs, making it difficult

to have similar and comparable criteria from survey to survey (Fig. 5). Densities around 6 GCPs per hectare resulted appropriated for low-altitude flights performed in the present work. However, appropriate GCPs density depends on the flight altitude, decreasing with the increase in height.[35,37] These authors found appropriate GCPs densities comparable to this study if all settings were taken into account (e.g., flight altitude and size of the survey area).

Other factors impacting the quality of the results include sun-related parameters (solar radiation and sun altitude) and parameters related to the characteristics of the surveyed area (e.g., the vegetation cover and terrain slope).

Usually, the impact of the sun is considered when acquiring reflection coefficient data. However, the tests performed here allowed us to verify that sun-related parameters can also affect the quality of topographic maps. It was found that the best conditions to fly coincide with sun altitudes between 30 and 40 deg and solar radiation per hour between 1750 and 2250 KJ/m^2 (Table 4 and Fig. 6). Values lower than the expressed ones represent low light conditions and induce high vRMSE variability. For instance, the decrease in the sun altitude is associated with an increase in the length of shadows, which makes it difficult to differentiate the objects in each image. Because the vRMSE increases with both solar radiation and sun altitude, values above the upper threshold also lead to lower accuracies. Higher solar radiation increases the brightness of the sand, decreasing the overall quality of the images.

The vegetation cover is sometimes mentioned as being responsible for affecting the final results of the DTMs.[38] The latter is related to the UAV-SfM approach, which cannot isolate the vegetation from the terrain.[9,11,23,24] Here, the possible effect of vegetation cover density on the quality of DSMs, as a previous product of a DTM, was evaluated; it was found that this factor appears to not affect the accuracy of the DSM [Fig. 9(a)]. This is probably due to the sparse and low vegetation that dominates the surveyed plots. However, changes in vegetation cover through time (e.g., end of spring and beginning of autumn) may induce erroneous estimates of dune topography as they could be interpreted as accumulation or erosion. Finally, the influence of the slope of the dune was also evaluated as this factor has been suggested to have a significant impact.[39,40] The results from the present work indicate that the vRMSE proportionally increases with the slope of the dune, with better results at gentle slopes [Fig. 9(b)]. This is due to the limitation of the SfM to correctly reproduce sudden changes in slope, i.e., if the terrain presents a high elevation variability in a short distance, the final DEM will not represent it accurately, and the vRMSE will increase.

5 Conclusions

The UAV-SfM approach has been increasingly used to monitor coastal dunes in recent years, and it has been proven to be a cost-efficient methodology. However, the accuracy of the results must be considered to optimize the quality of the survey results. This study explores the best combination of parameters relevant to the UAV-SfM survey to reduce vertical errors and improve the accuracy of UAVs-SfM products that can be easily replicated at any coastal dune area and other environments with similar characteristics and where high accuracy is desired. The present work proves that high accuracies (around 0.04 m) can be obtained flying at low altitudes and using a low-cost UAV (Mavic 2 Pro). For that, the flights must be planned to assure that the following criteria are met: overlapping of perpendicular flights; distribution of at least 6 GCPs per ha dispersed regularly in a diamond grid (covering the whole survey area); and flying when sun altitude is between 30 and 40 deg with a total solar radiation per hour between 1750 and 2250 KJ/m^2. The terrain slope was found to affect the quality of the results, with better results for dunes with gentle slopes. However, the quality of the results can be maintained when surveying high slope areas and slope breaks if the density of GCPs is increased.

Acknowledgments

The first author was supported by the Portuguese Foundation of Science and Technology (FCT) (Grant No. SFRH/BD/144869/2019). The fieldwork and processing data were supported by the research projects ENLACE, ON-OFF, and EW-COAST (Grant Nos. PTDC/CTA-GFI/28949/2017, PTDC/CTA-GEO/28941/2017, PTDC/CTA-OHR/28657/2017), funded by FCT.

Susana Costas and the overall work were supported under project No. UID/0350/2020 granted to CIMA by the FCT. Meteorological data were obtained from the Faro meteorological station maintained by the Portuguese Institute for Sea and Atmosphere, I. P. (IPMA, IP). The authors also acknowledge Direção Geral do Território the availability of the LiDAR survey from 2011 and the Instituto da Conservação da Natureza e das Florestas (ICNF, IP) and Capitania de Faro for the authorization to use the UAV at the study area. The authors also acknowledge the two unknown reviewers for their comments that largely helped to improve the manuscript. The authors declare that they have no known competing financial interests or personal relationships that could have appeared to influence the work reported in this paper.

Data availability statement

The data that support the findings of this study are available from the corresponding author, L. Bon de Sousa, upon reasonable request.

References

1. N. Elko et al., "Dune management challenges on developed coasts," *Shore Beach* **84**, 1–14 (2016).
2. M. Everard, L. Jones, and B. Watts, "Have we neglected the societal importance of sand dunes? An ecosystem services perspective," *Aquat. Conserv. Mar. Freshw. Ecosyst.* **20**, 476–487 (2010).
3. H. Karunarathna et al., "Multi-timescale morphological modelling of a dune-fronted sandy beach," *Coast. Eng.* **136**, 161–171 (2018).
4. I. J. Walker et al., "Scale-dependent perspectives on the geomorphology and evolution of beach-dune systems," *Earth-Sci. Rev.* **171**, 220–253 (2017).
5. B. Le Mauff et al., "Coastal monitoring solutions of the geomorphological response of beach-dune systems using multi-temporal LiDAR datasets (Vendée coast, France)," *Geomorphology* **304**, 121–140, (2018).
6. F. M. Scarelli et al., "Seasonal dune and beach monitoring using photogrammetry from UAV surveys to apply in the ICZM on the Ravenna coast (Emilia-Romagna, Italy)," *Remote Sens. Appl. Soc. Environ.* **7**, 27–39 (2017).
7. Y. Taddia et al., "UAVs to assess the evolution of embryo dunes," *Int. Arch. Photogramm. Remote Sens. Spatial Inf. Sci. - ISPRS Arch.* **XLII-2/W6**, 363–369 (2017).
8. J. A. Gonçalves and R. Henriques, "UAV photogrammetry for topographic monitoring of coastal areas," *ISPRS J. Photogramm. Remote Sens.*, **104**, 101–111 (2015).
9. Q. Laporte-Fauret et al., "Low-Cost UAV for high-resolution and large-scale coastal dune change monitoring using photogrammetry," *J. Mar. Sci. Eng.* **7**, 63 (2019).
10. M. R. James et al., "Optimising UAV topographic surveys processed with structure-from-motion: ground control quality, quantity and bundle adjustment," *Geomorphology* **280**, 51–66 (2017).
11. F. Mancini et al., "Using unmanned aerial vehicles (UAV) for high-resolution reconstruction of topography: the structure from motion approach on coastal environments," *Remote Sens.* **5**, 6880–6898 (2013).
12. F. Agüera-Vega, F. Carvajal-Ramírez, and P. Martínez-Carricondo, "Assessment of photogrammetric mapping accuracy based on variation ground control points number using unmanned aerial vehicle," *Meas. J. Int. Meas. Confed.* **98**, 221–227 (2017).
13. I. L. Turner, M. D. Harley, and C. D. Drummond, "UAVs for coastal surveying," *Coast. Eng.* **114**, 19–24, (2016).
14. M. E. B. Van Puijenbroek et al., "Exploring the contributions of vegetation and dune size to early dune development using unmanned aerial vehicle (UAV) imaging," *Biogeosciences*, **14**, 5533–5549 (2017).
15. F. Clapuyt, V. Vanacker, and K. Van Oost, "Reproducibility of UAV-based earth topography reconstructions based on Structure-from-Motion algorithms," *Geomorphology* **260**, 4–15, (2016).

16. C. Gong et al., "Analysis of the development of an erosion gully in an open-pit coal mine dump during a winter freeze-thaw cycle by using low-cost UAVs," *Remote Sens.* **11**, 1356 (2019).
17. E. Guisado-Pintado and D. W. T. Jackson, "Multi-scale variability of storm Ophelia 2017: the importance of synchronised environmental variables in coastal impact," *Sci. Total Environ.* **630**, 287–301 (2018).
18. C. H. Hugenholtz et al., "Geomorphological mapping with a small unmanned aircraft system (sUAS): feature detection and accuracy assessment of a photogrammetrically-derived digital terrain model," *Geomorphology* **194**, 16–24 (2013).
19. A. P. Bastos et al., "UAV derived information applied to the study of slow-changing morphology in dune systems," *J. Coast. Res.* **85**, 226–230 (2018).
20. K. L. Cook, "An evaluation of the effectiveness of low-cost UAVs and structure from motion for geomorphic change detection," *Geomorphology*, **278**, 195–208 (2017).
21. S. Harwin and A. Lucieer, "Assessing the accuracy of georeferenced point clouds produced via multi-view stereopsis from Unmanned Aerial Vehicle (UAV) imagery," *Remote Sens.* **4**, 1573–1599 (2012).
22. J. G. Moloney et al., "Coastal dune surveying using a low-cost Remotely Piloted Aerial System (RPAS)," *J. Coast. Res.* **34**, 1244–1255 (2018).
23. A. M. Martínez-Graña et al., "Augmented reality in a hiking tour of the miocene geoheritage of the Central Algarve Cliffs (Portugal)," *Geoheritage* **9**, 121–131 (2017).
24. C. Nolet et al., "UAV-imaging to model growth response of marram grass to sand burial: implications for coastal dune development," *Aeolian Res.* **31**, 50–61 (2018).
25. D. Ortega-Terol et al., "Automatic hotspot and sun glint detection in UAV multispectral images," *Sensors (Switzerland)* **17**(10), 2352 (2017).
26. A. Zanutta, A. Lambertini, and L. Vittuari, "UAV photogrammetry and ground surveys as a mapping tool for quickly monitoring shoreline and beach changes," *J. Mar. Sci. Eng.* **8**, 52 (2020).
27. M. E. Hodgson and G. R. Morgan, "Modeling sensitivity of topographic change with sUAS imagery," *Geomorphology* **8**, 107563 (2020).
28. Ó. Ferreira et al., "An integrated method for the determination of set-back lines for coastal erosion hazards on sandy shores," *Cont. Shelf Res.* **26**, 1030–1044 (2006).
29. K. Kombiadou et al., "Bridging the gap between resilience and geomorphology of complex coastal systems," *Earth-Science Rev.* **198**, 102934 (2019).
30. Ó. Ferreira, "Morphodynamic impact of inlet relocation to the updrift coast: Ancão Peninsula (Ria Formosa, Portugal)," in *Coast. Sediments 2011-7th Int. Symp. Coast. Eng. and Sci. of Coast. Sediment processes.*, Miami, pp. 497–504 (2011).
31. S. Costas et al., "Geomorphology exploring foredune growth capacity in a coarse sandy beach," *Geomorphology* **371**, 107435 (2020).
32. D. A. Pliatsika, "Dimitra Alkisti Pliatsika Aeolian sediment transport potentials and dune evolution in Ancão Peninsula (Ria Formosa), Portugal," http://hdl.handle.net/10400.1/12356 (2018).
33. "AgiSoft PhotoScan Standard," (Version 1.7.2) (Software), Retrieved from http://www.agisoft.com/downloads/installer/ (2021).
34. https://www.suncalc.org/
35. P. Martínez-Carricondo et al., "Assessment of UAV-photogrammetric mapping accuracy based on variation of ground control points," *Int. J. Appl. Earth Obs. Geoinf.* **72**, 1–10 (2018).
36. Y. Taddia, F. Stecchi, and A. Pellegrinelli, "Coastal mapping using DJI phantom 4 RTK in post-processing kinematic mode," *Drones* **4**, 9 (2020).
37. L. Santos Santana et al., "Influence of flight altitude and control points in the georeferencing of images obtained by unmanned aerial vehicle," *Eur. J. Remote Sens.* **54**, 59–71 (2021).
38. E. Honkavaara et al., "Influence of solar elevation in radiometric and geometric performance of multispectral photogrammetry," *ISPRS J. Photogramm. Remote Sens.* **67**, 13–26 (2012).
39. J. Müller et al., "Accuracy assessment of airborne photogrammetrically derived high-resolution digital elevation models in a high mountain environment," *ISPRS J. Photogramm. Remote Sens.* **98**, 58–69 (2014).

40. M. Stark et al., "From consumer to enterprise grade: how the choice of four UAS impacts point cloud quality," *Earth Surf. Process. Landforms* **46**, 2019–2043 (2021).

Luísa Bon de Sousa received her MSc degree in marine and coastal systems from the University of Algarve (Faro, Portugal) and is currently enrolled in the PhD program on marine, earth, and environmental sciences from the same university. Her PhD research topics are related to the evolution of coastal dunes and their drivers. She is also an expert on the use of UAVs and their use for coastal evolution assessment.

Susana Costas is an assistant researcher working at the Centre for Marine and Environmental Research (CIMA) at the University of Algarve. She received her MSc degree in coastal geosciences from the marine sciences department at the University of Vigo and her PhD in marine geosciences. Her research explores the geomorphological evolution of sandy coasts across different temporal scales, integrating the entire beach-dune profile and associated processes and risks to coastal communities.

Óscar Ferreira is an associate professor at the University of Algarve holding an MSc degree in geology and a PhD in marine sciences—Coastal Dynamics. He researches and teaches coastal dynamics and coastal risks. He is a member of the direction board of the MSc in coastal hazards and the BSc in marine and coastal management, and he was the head of the PhD on marine, earth, and environmental sciences and the MSc on marine and coastal systems.